2021

Temporal variability of downward fluxes of organic carbon off Monterey Bay

Castro, Carmen G.; Pennington, J. Timothy; Chavez, Francisco P.; Durazo, Reginaldo; Collins, Curtis A.

Deep-Sea Research Part II 151 (2018) 89–101

Contents lists available at ScienceDirect

Deep-Sea Research Part II

journal homepage: www.elsevier.com/locate/dsr2

Temporal variability of downward fluxes of organic carbon off Monterey Bay

Carmen G. Castro[a,*], Francisco P. Chavez[b], J. Timothy Pennington[b], Reginaldo Durazo[c], Curtis A. Collins[d]

[a] Consejo Superior de Investigaciones Científicas, Instituto de Investigaciones Marinas, E-36208 Vigo, Spain
[b] Monterey Bay Aquarium Research Institute, Moss Landing, CA 95039, USA
[c] Facultad de Ciencias Marinas, Universidad Autónoma de Baja California, Ensenada, Baja California, Mexico
[d] Department of Oceanography, Naval Postgraduate School, Monterey, CA 93943, USA

ARTICLE INFO

Keywords:
Vertical fluxes
Organic carbon
Coastal upwelling
Monterey Bay
California Current System
Annual variability
36.6°N
122.4°W

ABSTRACT

Sediment traps were deployed at two depths (300 m and 1200 m) off Monterey Bay (36°40′N and 122°25′W, Central California) for 7.3 years (1998–2005). The sediment trap data provided information about the quantity and quality of settling material, and allowed exploration of the relationship of the sinking material with the environmental conditions in this coastal upwelling region. The magnitude and composition of the settling material were highly variable over time. Organic carbon (C_{org}) fluxes ranged between 4–296 mg C m^{-2} day^{-1} and 0.1–142 mg C m^{-2} day^{-1} for shallow and deep sediment traps, respectively. The time series of C_{org} vertical flux was characterized by pulses of intense fluxes that were associated with peaks of primary production, generally during upwelling periods. Despite considerable variability, fluxes varied seasonally with highest values during the upwelling season and the lowest in winter. Attenuation of C_{org} vertical fluxes with depth (300 m vs. 1200 m) varied between 31% and 24% except for the late upwelling period, when there was an increase with depth likely due to resuspension of material from Monterey Canyon. Calculation of a seasonal vertical budget of organic carbon off Monterey Bay resulted in a transfer between 4.0% and 4.9% of the primary production to the deep ocean, suggesting that coastal upwelling efficiently sequestered CO_2.

1. Introduction

The biological pump, including all processes through which photosynthetically produced organic matter is transported from surface waters to the deep ocean (Volk and Hoffert, 1985), plays an important role in the global ocean carbon cycle. The biological pump is the main mechanism for removing CO_2 from the atmosphere and sequestering it in the deep sea (Gruber and Sarmiento, 2002; Passow and Carlson, 2012). The rate that the biological pump sequesters CO_2 is of key importance for the Earth's climate regulation (Sigman and Boyle, 2000; Riebesell et al., 2009; IPCC, 2013).

Carbon fixed by primary production is transferred to the deep ocean principally by (1) passively sinking particles, (2) vertical mixing of dissolved organic matter and (3) active transport by animals (Ducklow et al., 2001; Turner, 2015). Sinking particles constitute the main vector of downward transport of carbon (Sigman and Boyle, 2000; Buesseler et al., 2007), accounting for up to 80% of the carbon reaching the deep sea (Hansell, 2002; Hopkinson and Vallino, 2005). While sinking through the water column, there is a substantial attenuation of the particulate organic carbon (C_{org}) flux with the majority of the sinking C_{org} lost between 100 m and 500 m (Martin et al., 1987) due to remineralization (which converts it back to dissolved carbon dioxide) and solubilization processes (Martin et al., 1987; Steinberg et al., 2008). There is large variability in export of organic matter from the euphotic zone (export flux). The export flux averages 30% of net primary production in polar regions but is much lower, < 10% of net primary production, at low latitudes (Antia et al., 2001; Henson et al., 2011). Following De La Rocha and Passow (2007), the efficiency of the biological pump is here taken as the proportion of export flux that reaches the base of the mesopelagic zone (~ 1000 m). Sinking material that

Abbreviations: C_{org}, particulate organic carbon; C_{inorg}, particulate inorganic carbon; N, nitrogen; EU, early upwelling, February to April; LU, late upwelling, May to July; OC, oceanic, August to October; DV, Davidson, November to January; RCM, recording current meter; ADCP, acoustic Doppler current profiler; IRS, indented rotated sphere

* Corresponding author.
E-mail address: cgcastro@iim.csic.es (C.G. Castro).

https://doi.org/10.1016/j.dsr2.2018.07.001

Available online 03 July 2018

reaches this depth is effectively removed from interaction with the atmosphere for more than 100 years (Lampitt et al., 2008) and is considered 'sequestered'. This sequestration flux typically constitutes 6–25% of net primary production (Honda et al., 2002; Passow and Carlson, 2012).

Continental margins play a key role in the cycling of organic matter (Walsh, 1991; Falkowski et al., 1988; Liu et al., 2010; Bauer et al., 2013). Despite covering < 15% of the total ocean surface, about 27–30% of ocean CO_2 uptake from the atmosphere occurs within the continental margins (Chen and Borges, 2009). Some portion of this carbon uptake at the continental margin is ultimately exported to the deep sea or buried in margin sediments via the coastal (biological and solubility) pump. On the other hand, combining satellite annual global net primary production estimates with an empirical model of C_{org} sequestration, Muller-Karger et al. (2005) calculated that much more carbon sequestration takes places at continental margins (> 40%). These large uncertainties remain due to the variety of food webs and biogeochemical transformations inherent to these coastal marine ecosystems (Inthorn et al., 2006; Liu et al., 2010).

Among margins, coastal upwelling regions constitute an extreme case as they are among the most productive marine ecosystems in the world. Despite covering < 1% of the global ocean surface, they support about 5% of global marine primary production (Carr, 2003) and thus play a significant role in the biological pump on a global scale. Central California is one of these coastal upwelling regions, with prevailing northwesterly wind driven upwelling through spring and summer and favoring high primary production levels (Pennington and Chavez, 2000; Chavez et al., 2011). Pilskaln et al. (1996) assessed the fate of the organic carbon fixed in Monterey Bay (Central California) based on a 3-year time series of sediment trap data at 450 m and using previous measurements of benthic fluxes to indirectly calculate the organic carbon flux at the base of the mesopelagic. They estimated that on an annual basis, 1.6% of this production reached the seafloor while 81% of the net primary production was exported offshore by Ekman transport.

In this manuscript, the vertical flux of organic matter collected by sediment traps at 300 m and 1200 m depth in the coastal upwelling zone off Central California, from February 1998 to July 2005, were analyzed. Our goals are to (1) determine the seasonal and interannual variability of vertical flux of organic carbon, (2) estimate seasonal organic carbon budgets and (3) discuss the efficiency of coastal upwelling in sequestering CO_2 on the basis of particulate organic matter fluxes.

2. Material and methods

2.1. Study site

Monterey Bay, located in Central California, is a large open bay bisected by the Monterey Submarine Canyon, which runs east to west through the middle of the Bay (Fig. 1). Off Central California, hydrodynamic and biogeochemical variability is largely controlled by northwesterly winds that are in part responsible for the California Current and generate coastal upwelling (Strub et al., 1987; Pennington and Chavez, 2000; Collins et al., 2003). Based on thermohaline and biogeochemical properties for the coastal zone, inshore of the California Current, Pennington and Chavez (2000) defined four seasonal periods (1) spring (early) and (2) summer (late) upwelling seasons, from February to April and from May to July, respectively; (3) a fall (oceanic) season from August to October and (4) a winter (Davidson) period from November to the following January. Surface waters are cold and salty during early upwelling (EU) and warm during late upwelling (LU), remain warm but freshen in the oceanic (OC) season and cool again for the Davidson (DV) season. The EU and LU seasons exhibit the highest surface nutrients and primary production, mainly due to diatom blooms. During these seasons, the biologically productive waters extend several hundred kilometers from shore, to the inshore edge of the California Current (Collins et al., 2003). Phytoplankton blooms, primarily composed of oceanic picoplankton, continue to develop intermittently for the OC season. In fact, during this season there is an onshore shift of the California Current, about 80 km toward shore. During the DV season, primary production is low, regulated by low levels of nitrate, light and temperature.

2.2. Sample collection

2.2.1. Cruises

Station M2, near the mouth of Monterey Bay (Fig. 1), has been occupied bimonthly since 1993 as part of the Monterey Bay Time Series (Chavez et al., 2002). In this study, observations took place between 1998 and 2006. Methods used to collect hydrographic data were given by Asanuma et al. (1999). Methods for biological and chemical measurements have been described by Pennington and Chavez (2000). Briefly, a SeaBird 911 CTD was used for collecting the hydrographic data to at least 200 m and Niskin bottle samples for nutrients, chlorophyll a and primary production were obtained from the sea surface to 200 m during each cast. Nutrient samples were frozen unfiltered aboard ship and later processed on an AlpChem autoanalyzer (Sakamoto et al., 1990). Primary production (PP) was measured by ^{14}C uptake in 24 h in situ incubations (Pennington and Chavez, 2000). Water column-integrated PP was calculated by using trapezoidal integrations of PP over the euphotic zone.

2.2.2. Mooring deployment

From 1998 to 2006, a mooring designated S2, was deployed on the continental slope near M2 at 36°40′N and 122°25′W and 1800 m depth (Fig. 1). The mooring included an upward looking 300 kHz RD Instruments ADCP at 300 m depth, two current meters at 305 m and 1200 m depth and two sediment traps just below each current meter. Deployments lasted for five to six months except the last deployment which was for 10 months (Table 1). In the following sections, measurements at the upper (lower) level will be referred to as "300 m" ("1200 m") nominal depth.

Aanderaa recording current meters (RCM8) were used. Current speed was measured by rotations of a shrouded paddle-type rotor which was magnetically linked to an electronic counter and current direction was measured by magnetic compass. Before deployment, the compass was calibrated and the counter tested for accuracy and proper operation in the laboratory. Both the RCM8 and ADCP measured pressure and temperature and the ADCP measured pitch and roll as well. The RCM8 recorded vector averaged speed and direction at 30 min intervals. Further details regarding current measurements are given by Aguilar-Morales (2003).

Two sequential sediment traps were used in this study (Table 1). One was an Indented Rotating Sphere (IRS) sediment trap (Peterson et al., 1993) which was deployed at 320 m. The second was a Honjo Mark VI sediment trap (Honjo and Doherty, 1988) at ~ 1205 m. Traps were pre-programmed to sample the fluxes of sinking particles over approximately 14 days for all deployments except the last, for which the sampling interval was 28 days. Gaps in the sediment trap time-series were due to technical issues related to failure of the sediment trap program as well as analytical issues described in the following section. All sediment traps were thoroughly acid-cleaned before the deployment. In the laboratory, the rotary collector was cleaned with detergent, soaked in HCl overnight, and rinsed several times with distilled water. Once at sea, the traps were rinsed with seawater. The receiving cups were filled with seawater with a NaCl excess of 5 g L^{-1} and poisoned with 3.0 mM of mercury chloride to avoid degradation of collected particles and disruption by swimmers (including organisms that did not fall gravitationally through the water column; Thunell et al., 2000). Upon recovery, the receiving cups were stored in the dark at 4 °C until they were processed.

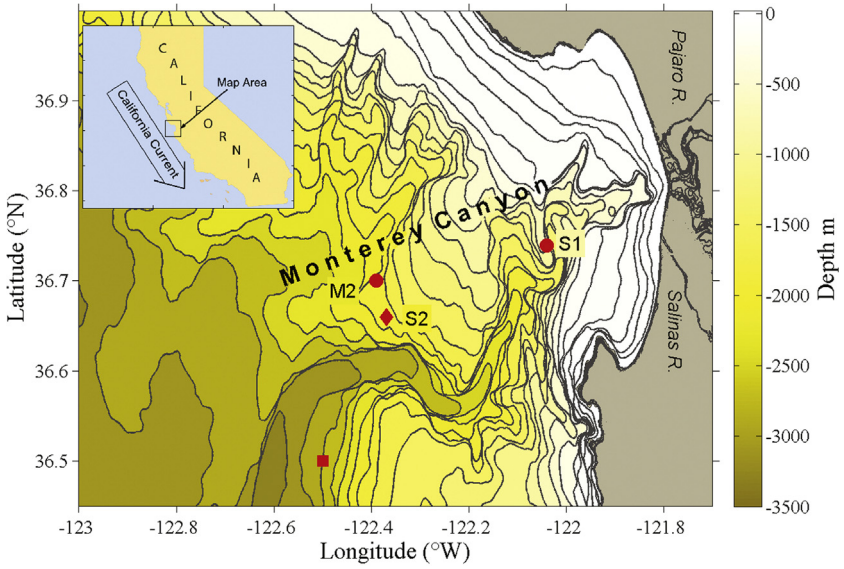

Fig. 1. Chart (in m) of Monterey Bay and the location of M2, S1 and S2 moorings. The position at which Ekman transports were estimated is shown by a red square.

Table 1
Sediment trap deployment period, trap type, sampling interval and specific comments.

Deploy	Sampling period		Trap Type	Interval
	Start yy/mm/dd	Finish yy/mm/dd		
300 m				
01	98/03/25	98/08/21	IRS	10 × 14, 1 × 9
02	98/08/26	99/01/27	IRS	11 × 14
03	99/02/10	99/07/14	IRS	11 × 14
04	99/08/04	00/01/05	IRS	11 × 14[a]
05	00/02/09	00/07/12	IRS	11 × 14
06	00/08/16	01/01/03	IRS	11 × 14[b]
07	01/01/31	01/07/04	IRS	11 × 14[b]
08	01/08/22	02/01/23	IRS	11 × 14
09	02/02/08	02/07/10	IRS	10 × 14, 1 × 9
10	02/09/04	03/02/05	IRS	11 × 14
11	03/03/12	03/08/13	IRS	11 × 14
12	03/09/10	04/02/11	IRS	11 × 14[c]
13	04/03/17	04/08/18	IRS	11 × 14
14	04/09/13	05/06/20	IRS	10 × 28
1200 m				
01	98/03/25	98/08/21	Mark VI	10 × 14, 1 × 9
02	98/08/26	99/01/13	Mark VI	10 × 14
03	99/02/10	99/07/14	Mark VI	12 × 14[d]
04	99/08/04	00/01/19	Mark VI	12 × 14
05	00/02/09	00/07/12	Mark VI	11 × 14[e]
06	00/08/02	01/01/17	Mark VI	12 × 14[a]
07	01/01/31	01/07/04	Mark VI	12 × 14[f]
08	01/08/22	02/02/06	Mark VI	12 × 14
09	02/02/08	02/08/07	Mark VI	12 × 14, 1 × 12
10	02/09/04	03/03/05	Mark VI	13 × 14
11	03/03/12	03/08/27	Mark VI	12 × 14
12	03/09/10	04/03/10	Mark VI	13 × 14
13	04/03/17	04/09/01	Mark VI	12 × 14
14	04/09/13	05/06/20	Mark VI	10 × 28

[a] Insufficient material for the last 5 samples.
[b] Insufficient material for the last 4 samples.
[c] Program failed; missing all samples.
[d] Battery failed; missing all samples.
[e] Program failed; missing last 6 samples.
[f] Material clogged; missing last 8 samples.

2.3. Sample processing and analytical techniques

In the laboratory, swimmers were removed from the samples by using fine tweezers under a dissecting microscope. When necessary, the samples were divided into aliquots using a high-precision wet sample divider (Mc Lane-WSD-10). The WSD-10 divided a wet particle sample into five or ten equal splits. To remove salts, the splits were rinsed with cold distilled water, centrifuged and the supernatant eliminated. Samples were then dried in a 60 °C oven for 24 h. Dry splits were firstly used to calculate total mass fluxes. For total and organic carbon and nitrogen elemental composition analysis, approximately 20 mg subsamples of dry split were used. Subsamples for organic carbon were first decarbonated with repeated additions of 50 µL of HCl 15%. Total and organic carbon and nitrogen were measured with a Carlo-Erba NA-1100 analyzer. Sample analysis errors were generally 1% for carbon and nitrogen content. For a few periods, sample material was not sufficient for analysis (Table 1). For IRS samples of deployments no. 7 and 10, there were no samples due to analytical problems. Assuming all the inorganic carbon was calcium carbonate ($CaCO_3$), the $CaCO_3$ content was estimated as [(total carbon – organic carbon) × 8.33].

2.4. Offshore Ekman transport

Offshore Ekman mass transport per meter of coastline, kg m^{-1} s^{-1}, was used as an index of strength of upwelling (Schwing et al., 1996). The offshore transport estimate was based upon 6-h charts of synoptic weather produced by the U.S. Navy Fleet Numerical and Oceanography Center. The Ekman transports (and wind stress curl) were downloaded from http://upwell.pfeg.noaa.gov/erddap/griddap/erdlasFnWPr.html for 36.5°N, 122.5°W (location shown on Fig. 1) from 1998 to 2005. Missing values were replaced by linear interpolation, and rotated so that offshore (negative) transport was directed perpendicular to the coast (toward 240 °T).

3. Results

3.1. Monterey Bay time series

The time series of offshore Ekman transport, temperature, salinity, nitrate and primary production in the upper 200 m for the period 1998–2005 are shown for station M2 in Fig. 2. Time series of Ekman transport (Fig. 2A) clearly marked the upwelling season between February and September. In addition, there was large interannual variability also seen in the thermohaline and biogeochemical properties. The most negative (offshore) Ekman transport occurred during the 1999 La Niña event and the maximum (onshore) during the 1998 El Niño event (Fig. 2A). In fact, the most intense downwelling favouring winds were

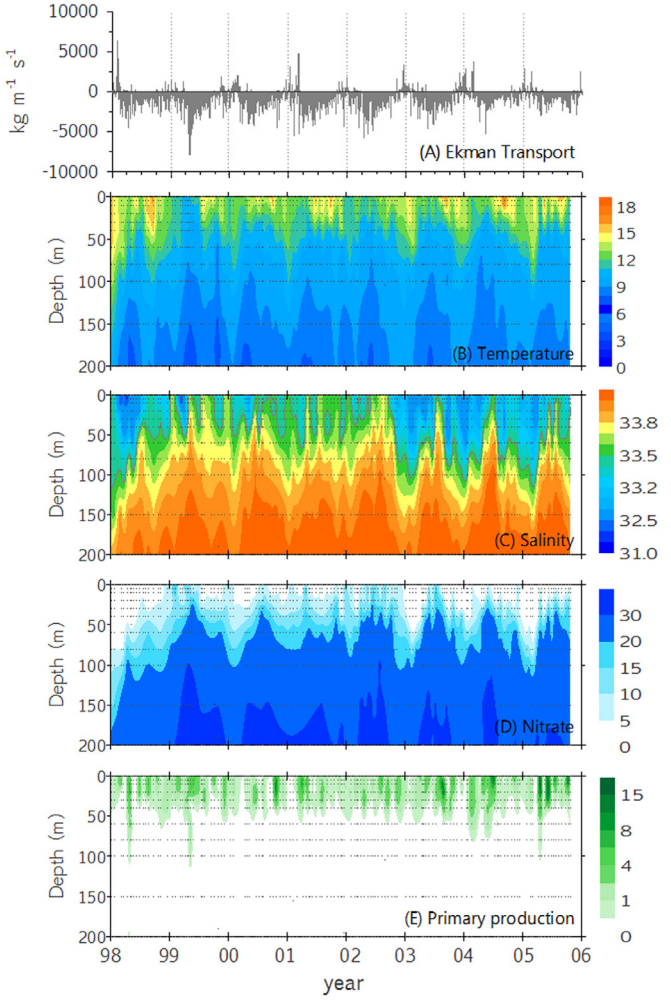

Fig. 2. Time series of (A) across shore Ekman transport at 36.5°N, 122.5°W (kg m^{-1} s^{-1}); negative values indicate offshore transport associated with coastal upwelling. Time series for the upper 200 m at the M2 site (shown in Fig. 1): (B) temperature (°C), (C) salinity, (D) nitrate (μM) and (E) primary production (mg C m^{-3} day^{-1}).

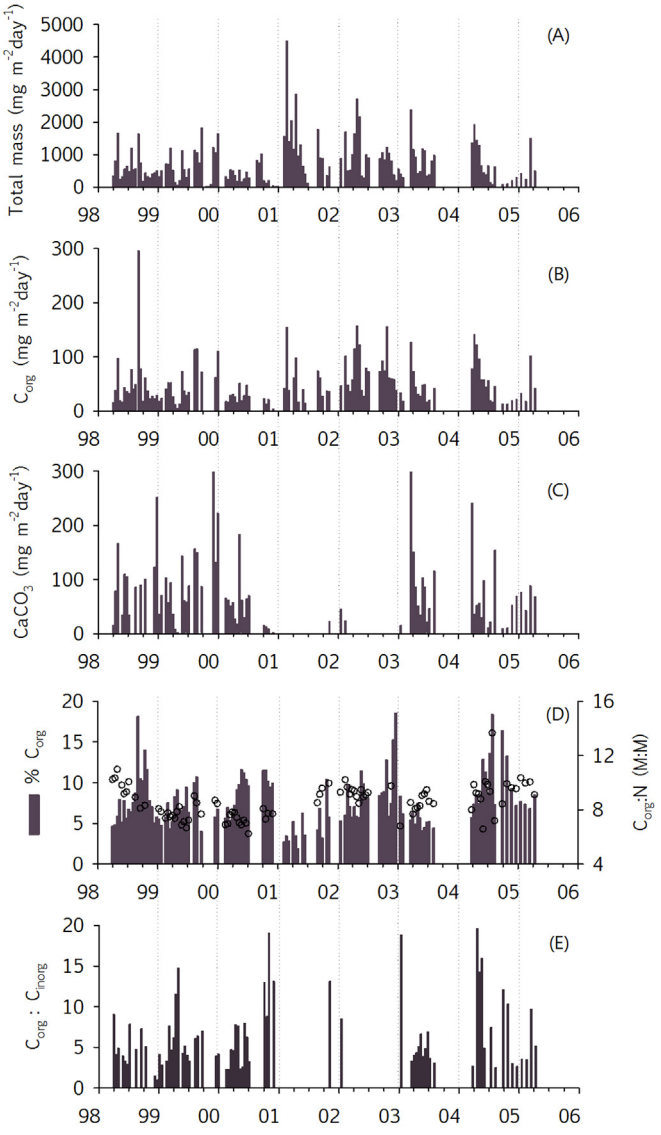

Fig. 3. Time series of fluxes of (A) total mass, (B) C_{org}, (C) $CaCO_3$, (D) %C_{org} relative to total mass and C_{org}:N ratio (open circles) and (E) C_{org}: C_{inorg} ratio at 300 m.

observed at the beginning of 1998, during El Niño.

Despite the large interannual variability in water column temperature, mostly due to the warm 1998 El Niño and the cold 1999 La Niña, there was also marked seasonality for the study years (Fig. 2B). For each year, lowest temperatures at the sea surface were reached between March and April (< 12.0 °C) and were warmest between July and September (> 13.5 °C). However, year 2000 was characterized by relatively homogenous temperature (12.5 ± 1.1 °C) in the upper 50 m of the water column for the entire year.

The salinity time series consisted of an annual cycle modulated by large interannual variability (Fig. 2C). The 1998 El Niño and 1999 La Niña years were both characterized by large salinity variability at the sea surface, ranging from a minimum of 32.2 in March of both years and maximum of 33.5 (33.7) in May 1998 (July 1999), decreasing slightly, 0.1 (0.2), for October. However, from 2000 to 2002, sea surface salinity values were nearly homogeneous and relatively salty for the entire year (33.51 ± 0.14), except for the last four months of 2002. In fact, there was a sharp decrease in salinity with a deepening of the halocline in September of 2002 through 2005, so that upper ocean salinities were lower (< 33.2) than previous years.

The strong perturbation of the 1997–1998 El Niño was easily identified in the nitrate time series (Fig. 2D) by low nitrate levels (< 5 μM) and a deep nitracline for the entire year. For other years, high nitrate levels reaching the upper levels of the water column were registered during the upwelling season though with interannual differences. In 2002, nitrate levels higher than 10 μM persisted for the entire upwelling season. In contrast, nitracline depth did not outcrop and reached only 20 m depth in May 2000.

Primary production values tracked thermohaline and chemical conditions (Fig. 2E). The annual maximum values of primary production were observed during the upwelling season, mainly during March–September, and minimum values during winter. There was also large interannual variability and during the last three years relatively higher primary production values were observed including the remarkably large value of integrated primary production of 228 mg m^{-2} day^{-1} (not shown) in the photic zone during August 2003.

3.2. Monterey Bay vertical flux time series

The complete time series of total mass, organic carbon (C_{org}) and $CaCO_3$ observed from 1998 through 2005 at 300 m and 1200 m depth are presented in Figs. 3 and 4. At 300 m depth, total mass flux varied from a minimum value of 22.1 mg m^{-2} day^{-1} to a maximum of 4502 mg m^{-2} day^{-1} (Fig. 3A) The mean downward flux averaged over

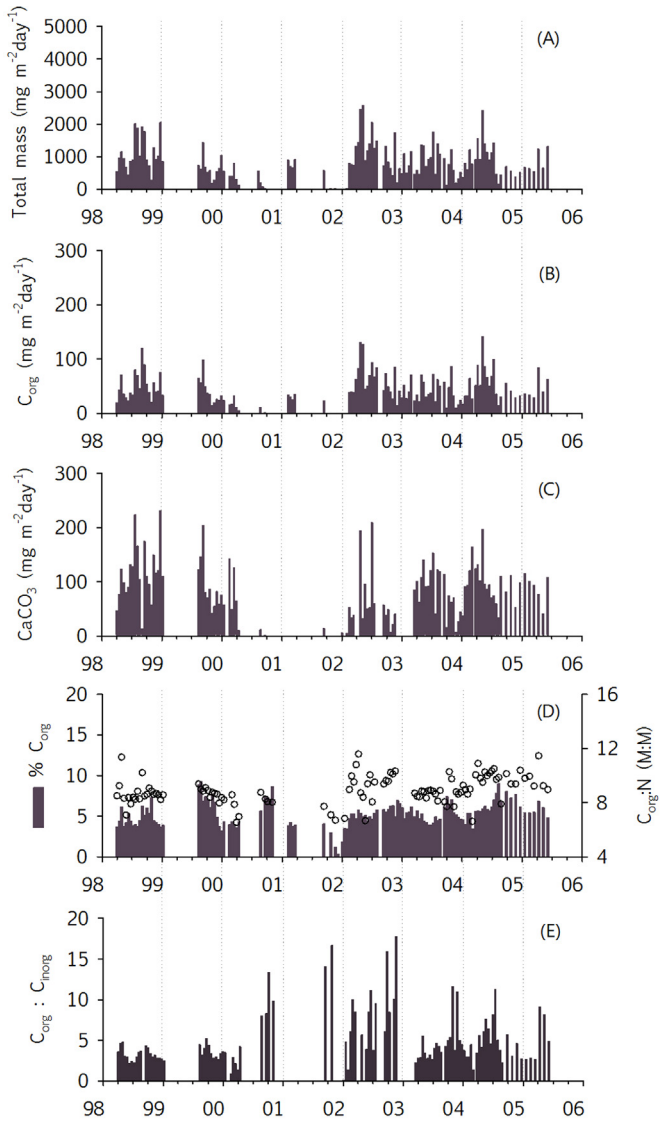

Fig. 4. Time series of fluxes of (A) total mass, (B) C_{org} and (C) $CaCO_3$, (D) $\%C_{org}$ relative to total mass and C_{org}:N ratio (open circles) and (E) C_{org}: C_{inorg} ratio at 1200 m.

the entire study period was 762 ± 660 mg m^{-2} day^{-1}. Organic carbon fluxes ranged between a minimum of 4.1 mg m^{-2} day^{-1} and a maximum value of 296 mg m^{-2} day^{-1} for September 1998, with an average flux for the entire study period of 52 ± 41 mg m^{-2} day^{-1} (Fig. 3B). In general, maximum peaks of C_{org} flux which occurred at the same time as maximum values of primary production occurred during the EU season from February to April (April 1998, May 1999, April 2001, April 2002, March 2003, April 2004, March 2005). However, there were other maximum pulses of C_{org} flux not associated with maximum values of primary production, as in December 1999, February 2001, February 2002 and October 2002. Fluxes of C_{org} followed a similar temporal trend to total mass fluxes with a Pearson correlation coefficient of 0.77. Temporal variability of $CaCO_3$ flux was similar to C_{org} flux, with an average of 75 ± 62 mg m^{-2} day^{-1} for the entire study period (Fig. 3C). Although $CaCO_3$ fluxes corresponded to variations in C_{org} and total mass fluxes (r = 0.51 and 0.52 respectively), there were some peaks of C_{org} flux not reflected by $CaCO_3$ pulses as in September 1998, February 2002, April 2004 and March 2005. Likewise, there were other peaks in $CaCO_3$ fluxes that occurred simultaneously with lower fluxes of C_{org} such as observed in December 1998 and May 2000.

At 1200 m depth, total mass flux varied from a minimum value of 0.2 mg m^{-2} day^{-1} to a maximum of 2580 mg m^{-2} day^{-1} (Fig. 4A). Organic carbon fluxes varied between a minimum of 0.1 mg m^{-2} day^{-1} and maximum of 142 mg m^{-2} day^{-1}, with an average for the study period of 44 ± 28 mg m^{-2} day^{-1} (Fig. 4B). These fluxes followed a similar temporal evolution of C_{org} fluxes at 300 m, with a significant Pearson correlation coefficient of 0.47 between the two time series. In fact, maximum pulses of C_{org} at 1200 m corresponded to maximum pulses at 300 m, as observed in April 1998, September 1998, August 1999, April 2002, October 2002, April 2003 and April 2004. In contrast, maximum peaks of C_{org} at 300 m during the DV season from November to January (December 1999, February 2001 and February 2002) were not reflected in maximum peaks at 1200 m. At 1200 m fluxes of $CaCO_3$ (Fig. 4C) correlated with fluxes of total mass and C_{org} with Pearson correlation coefficients of 0.64 and 0.57, respectively.

Regarding the composition of settling material, the percentage of C_{org} relative to total mass for the shallower trap varied between a minimum of 1.8% and maximum value of 18.6%, with an average value of 7.8 ± 3.2% for the entire study period (Fig. 3D). The percentage of C_{org} in the deepest trap was significantly lower than for the shallower trap with an average value of 5.3 ± 1.5% (Fig. 4D). The highest percentages of C_{org} were registered during the OC season from August to October at both trap levels. The C_{org}:N molar ratio ranged from 6.2 to 13.7 (average 8.6 ± 1.2) at the shallower level (Fig. 3D). At 1200 m, average C_{org}:N molar ratio (8.9 ± 1.0) was not significantly different from the shallower trap (Fig. 4D).

3.3. Annual cycles

The mean annual cycle of wind-driven offshore Ekman transport for 1998–2005 is shown in Fig. 5A. The annual cycle accounts for 76% of the observed variance of the offshore Ekman transport. The mean annual cycle of Ekman transport is directed offshore for all but 19 days in late January when weak onshore transport occurs. Maximum (e.g. onshore) transport is 17 kg m^{-1} s^{-1} on January 20 and subsequently decreases monotonically to strongly negative (e.g. offshore) transport of − 1296 kg m^{-1} s^{-1} on June 3. It then takes seven and a half months for the winds to increase to their January maximum. Assuming a Rossby radius of 20 km, the minimum transport corresponds to an upwelling rate of 8 m day^{-1}. The seasonal variability and the annual cycles of the thermohaline properties, nitrate and primary production off Monterey Bay have been described in detail by Pennington and Chavez (2000), as previously mentioned. Note the two maxima in primary production (Fig. 5B) during the upwelling period, centred on April 15 and August 5.

The annual cycle of currents and temperature at 300 m illustrates the physical response to wind forcing at the location of the upper sediment trap (Fig. 5C–D). At the start of the year, the mean currents are directed poleward, and subsequently slow to 1 cm s^{-1} on March 19. The poleward flow then increases to a maximum velocity, 9.3 cm s^{-1}, on June 13, ten days after the offshore directed Ekman transport is greatest. The mean annual 300 m alongshore currents subsequently decrease to − 0.5 cm s^{-1} on October 10. Note that alongshore currents are directed poleward for all but 28 days which are centred on this minimum. The annual cycle of alongshore flow at 300 m accounts for 24% of the variability of the alongshore flow. Unlike Ekman transport, the alongshore current velocity has secondary minima and maxima. The mean annual cycle of temperature at 300 m (Fig. 5D) resembles the annual cycle of Ekman transport at the start of the year: the temperature is 7.8 °C on January 22 and subsequently decreases as the upwelling favorable transports increase. Minimum temperatures (7.1 °C) occurs on May 6, about a month before the offshore transport peaks, and subsequently reaches a maximum value of 7.8 °C on August 10, about 2 months after the poleward velocities are largest. The May cooling appears to be a response to upwelling, and the subsequent warming a response to the increasing strength of the poleward flow of equatorial waters. For temperature, the mean annual cycle accounts for 44.6% of

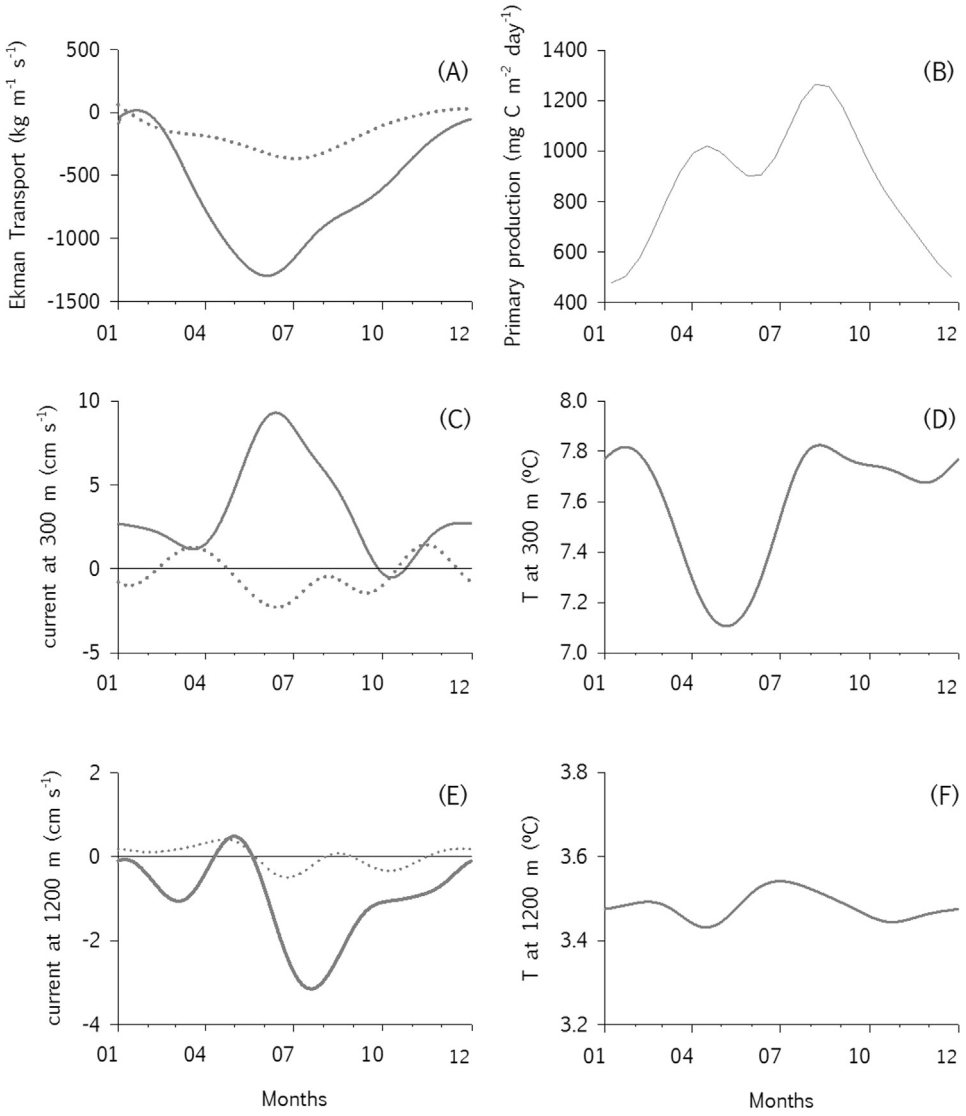

Fig. 5. Annual cycle of (A) across shore (solid line) and alongshore (dashed line) Ekman transport (kg m^{-1} s^{-1}), (B) integrated primary production in the photic zone (mg C m^{-2} day^{-1}), (C) alongshore (solid line) and across shore (dashed line) currents at 300 m (cm s^{-1}); positive alongshore (across shore) currents are directed toward 346°T (76°T), (D) temperature at 300 m (°C), (E) alongshore (solid line) and across shore (dashed line) currents at 1200 m (cm s^{-1}) and (F) temperature at 1200 m (°C).

the low frequency variability. The annual cycle of alongshore currents at 1200 m at S2 (Fig. 5E) are southward all year round except for a few days centred on May 5. Maximum southward speed is 3.1 cm s^{-1} on July 18, a few days after the maximum poleward current at 300 m. The annual cycle of temperature at 1200 m (Fig. 5F) only varied 0.11 °C for the entire year but this warming occurred between June 29 (minimum temperature 3.43 °C) and June 29 (maximum temperature 3.54 °C) about the same time the current accelerated to maximum southward flow.

For the settling material at the two sediment trap levels, seasonal averages are calculated for the four seasonal periods defined by Pennington and Chavez (2000) (Fig. 6). At 300 m, total mass flux is significantly higher during EU (1129 ± 929 mg m^{-2} day^{-1}; $p < 0.05$) compared with the other three seasons; while the lowest total mass flux corresponds to DV season (Fig. 6A). Organic carbon fluxes follow a slightly different seasonal pattern with significantly higher values during the EU and OC seasons (60 ± 43 mg m^{-2} day^{-1} and 68 ± 60 mg m^{-2} day^{-1} respectively) (Fig. 6B). Average seasonal fluxes of $CaCO_3$ do not show any significant differences amongst seasons (Fig. 6C). Due to the high total mass flux average for EU, the percent C_{org} for this season is significantly lower (6 ± 1%) than for other seasons (Fig. 6D), as discussed further in Section 4.3. Maximum average percent of C_{org} is 10 ± 4% during the OC season. The C_{org}:N and C_{org}:C_{inorg} ratio are not significantly different amongst the seasons and range from 8.5 ± 0.8–8.8 ± 1.1 (Figs. 6D) and 5.7 ± 3.5–7.2 ± 3.3 (Fig. 6E), respectively.

At 1200 m, seasonal particle fluxes of total mass and C_{org} are not the same as at 300 m (Fig. 6F–G). Maximum seasonal fluxes are found during the LU season from May to July (1194 ± 568 mg m^{-2} day^{-1} and 59 ± 31 mg m^{-2} day^{-1} for total mass and C_{org} respectively) and, as at 300 m, minimum values occur during the DV season (526 ± 495 mg m^{-2} day^{-1} and 28 ± 20 mg m^{-2} day^{-1} for total mass and organic carbon respectively). Likewise, maximum seasonal flux of $CaCO_3$ (101 ± 50 mg m^{-2} day^{-1}) occurs during the LU season but is only significantly different from the DV seasonal flux (Fig. 6H). Regarding the quality of settling material, as at 300 m, the highest C_{org} content is for the OC season (6 ± 1%); while C_{org}:N ratio is not significantly different for the four seasons (Fig. 6I). The seasonal average C_{org}: C_{inorg} ratio varies between 4.1 ± 2.4 for EU and 6.2 ± 4.1 for OC, being significantly different between these two seasons ($p < 0.05$) (Fig. 6J).

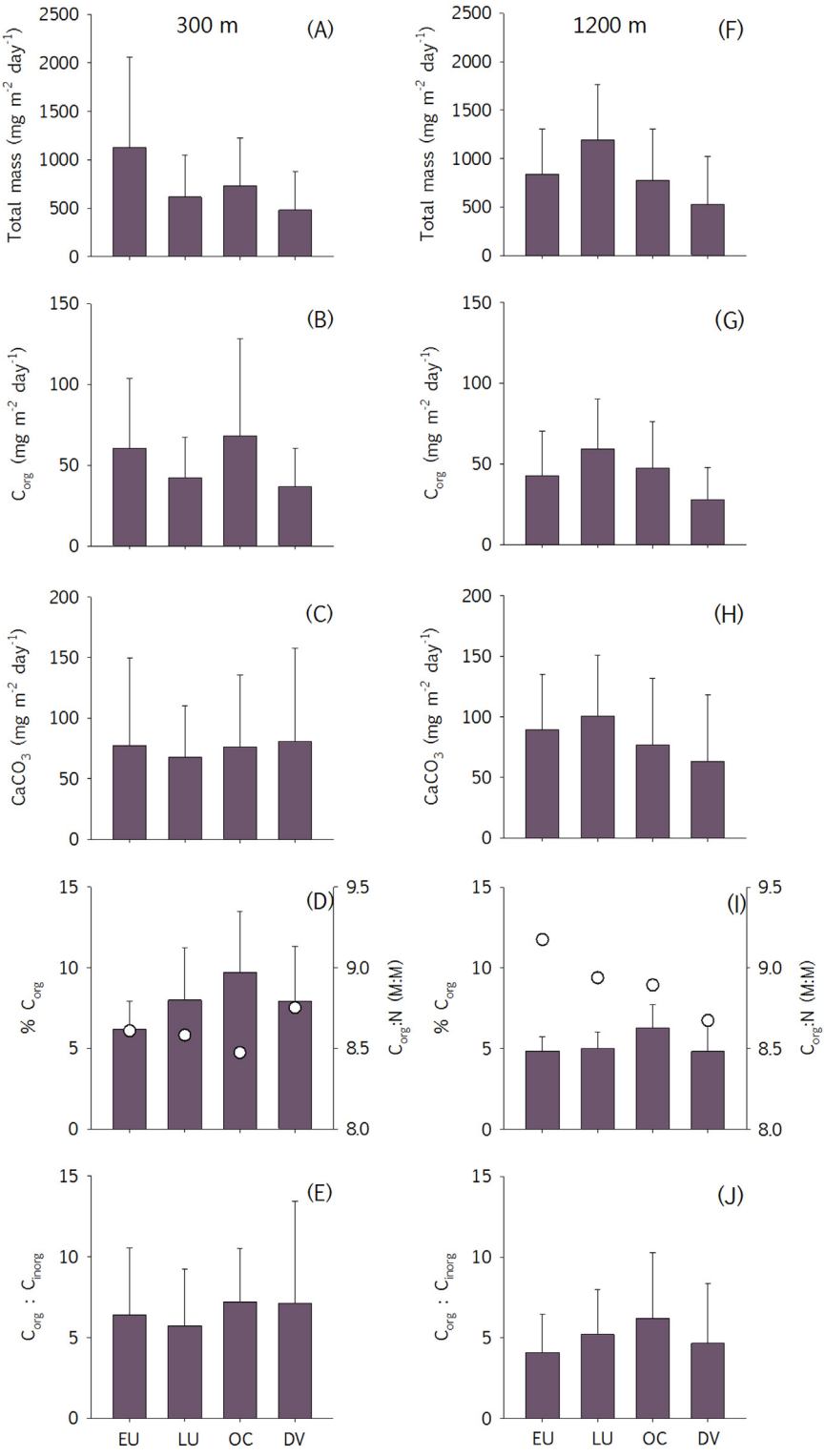

Fig. 6. Seasonal averages for (A) Total mass, (B) C_{org} and (C) $CaCO_3$, (D) $\%C_{org}$ relative to total mass and C_{org}:N ratio (open circles) and (E) C_{org}: C_{inorg} ratio at 300 m and (F) Total mass, (G) C_{org} and (H) $CaCO_3$, (I)$\%C_{org}$ relative to total mass and C_{org}:N ratio (open circles) and (J) C_{org}:C_{inorg} ratio at 1200 m. EU = early upwelling, February to April, LU = late upwelling, May to July, OC= oceanic, August to October, and DV = Davidson season, November to January.

4. Discussion

This study examines the biological pump offshore of Monterey Bay through 2 time series of vertical carbon flux as captured by sediment traps. A discussion of the efficiency of the deployed sediment traps is first presented. Subsequently, the discussion focuses on the vertical flux of C_{org} and its temporal (seasonal and interannual) and vertical (300 and 1200 m) variability to evaluate the fate of particulate organic carbon. Finally, a seasonal one dimensional (1D) budget of organic carbon in this coastal upwelling system is presented.

4.1. Quality of trap fluxes

The use of sediment traps has contributed significantly to the study

Table 2
Statistics of current speeds, cm s^{-1} at the two sediment trap depths (300 m and 1200 m) and frequency of time when mean currents > 15 cm s^{-1}. Seasons are defined as: EU is early upwelling, February to April, LU is late upwelling, May to July, OC is oceanic, August to October, and DV is Davidson season, November to January.

Year	Season	AVG 300 m	STD 300 m	v > 15 cm s^{-1} 300 m	AVG 1200 m	STD 1200 m
1998	EU	3.7	1.2	0%	1.75	0.86
1998	LU	12.4	4.0	33%	2.32	0.89
1998	OC	6.7	3.7	0%	2.16	1.57
1998	DV	7.0	5.1	0%	2.10	0.96
1999	EU	5.8	3.7	0%		
1999	LU	15.4	3.4	60%		
1999	OC	7.0	4.2	0%	3.16	1.88
1999	DV	7.2	2.7	0%	2.14	0.40
2000	EU	5.5	3.5	0%	1.24	0.63
2000	LU	14.5	7.6	40%		
2000	OC	13.3	4.0	40%	4.26	1.41
2000	DV	6.2	1.7	0%	3.48	1.21
2001	EU	6.7	4.6	0%	3.36	0.53
2001	LU	11.6	4.4	20%		
2001	OC	12.8	1.6	0%	2.48	0.74
2001	DV	7.8	3.4	0%	1.72	1.14
2002	EU	8.6	4.1	0%	1.90	1.33
2002	LU	13.2	5.2	20%	2.54	1.54
2002	OC	18.6	4.0	50%	3.70	2.10
2002	DV	8.5	2.8	0%	3.68	3.43
2003	EU	8.9	2.7	0%	4.02	3.43
2003	LU	13.3	3.9	33%	4.62	1.56
2003	OC	7.9	4.9	0%	2.82	1.40
2003	DV	6.0	2.3	0%	1.44	0.83
2004	EU	9.5	3.5	0%	3.73	2.54
2004	LU	11.3	6.2	29%	5.26	3.34
2004	OC	13.1	9.8	0%	3.58	1.25
2004	DV	6.5	2.8	0%	2.20	0.60
2005	EU	4.9	1.0	0%	1.94	1.80
2005	LU	13.5	1.1	0%	1.85	1.26

of vertical particulate matter flux in the oceans. However, trap collection efficiency has been questioned because of potential hydrodynamic bias due to current speed (Gardner et al., 1997; Buesseler et al., 2007), and associated errors due to trap tilting (Gardner, 1985). To address these issues, a brief quality assessment of the trap fluxes reported here is given below.

Gardner (1980) indicated that cylindrical traps, such as the IRS and Honjo Mark VI used here, experience a negligible reduction of collection efficiency of vertical fluxes in flows up to 15 cm s^{-1}. Subsequently, Gardner et al. (1997) found that in the field, cylindrical collectors with high aspect ratios (> 2) should produce little bias in current speeds as large as 22 cm s^{-1}. Average current speeds at 300 m for each season are shown in Table 2 with mean current speeds of 3.7–18.6 cm s^{-1}. Mean current velocities above 15 cm s^{-1} (Gardner, 1980; Antia et al., 1999; Heussner et al., 2006) were observed during the LU season of all years and during two OC seasons. During LU, the percentage of time with currents above 15 cm s^{-1} ranged between 20% in year 2002–60% during the La Niña year of 1999, when strong northerly winds were persistent. During the OC, only 2000 and 2002 experienced speeds above 15 cm s^{-1}. At 1200 m depth, average current speeds were much lower than 15 cm s^{-1}, ranging between 1.2 and 5.3 cm s^{-1} (Table 2). Following Gardner et al. (1997), if strong hydrodynamic biases due to current intensity had occurred, either high fluxes should be expected when currents were strong (overcollection) or, conversely, low fluxes when currents were weak (undercollection). However, correlation coefficients of total mass flux vs current speed for each of the four seasons were not statistically significant (r > 0.2); this indicated that particulate matter fluxes were not significantly biased by horizontal current speeds.

Trap inclination to the vertical can also affect trap efficiency (Gardner, 1985) but inclination was limited by mooring design. Fig. 7 shows the relationship between mooring tilt and current speed at 300 m for 15 min samples. The tilt angle was less than 0.8° at velocities ~ 40 cm s^{-1}, indicating that the sediment trap was very stable and that inclination probably did not affect efficiency

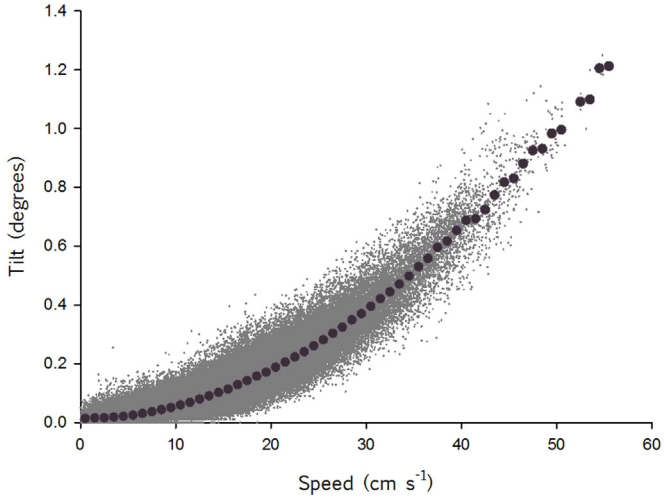

Fig. 7. Relationship between observed mooring tilt and current speed at 300 m at the S2 mooring. Grey dots are individual 15-min observations and dark grey dots are means of tilt observations for each 1 cm s^{-1} increment of speed.

Thus, even though high current speeds during the late upwelling season could have influenced the efficiency of the 300-m sediment trap, the very low inclination of the mooring line and the absence of correlation between mean current speed and mass of sinking material suggested that the sediment trap data were not biased by hydrodynamic effects.

4.2. Seasonal and interannual variability of the vertical fluxes

This 7.3-year study of particle flux off Monterey Bay spanned very different oceanographic conditions including (1) the last phase of the strong 1997–1998 El Niño, (2) the subsequent cold 1999–2000 La Niña, and (3) the anomalous onshore presence of Subarctic waters between 2002 and 2005. Although there were gaps in the sediment trap observations, the data provide insights about the vertical export organic carbon from the photic zone.

In general, C_{org} flux measured at station M2 40 km offshore of Monterey Bay (52 and 44 mg m^{-2} day^{-1} at 300 m and 1200 m respectively) were similar to those previously reported by Pilskaln et al. (1996) at station S1 at the mouth of Monterey Bay (40 mg m^{-2} day^{-1}; Fig. 1). For other coastal margins, Thunell et al. (2007) reported an average C_{org} flux in Santa Barbara Basin (~ 315 km south of Monterey Bay) of 96 mg m^{-2} day^{-1}, nearly twice that of Cariaco Basin and 4 times higher than Guaymas Basin, with all three sites having C_{org} flux significantly higher than the open ocean average (7 mg m^{-2} day^{-1} for the depth interval from 250 to 500 m).

Vertical fluxes of C_{org} off Monterey Bay were lowest during the DV season, though not significantly different from the LU season, and maxima for the EU and OC seasons at 300 m depth. This seasonal variation seemed to reflect biological control, and should be related to the seasonal cycle of primary production in the region in response to coastal upwelling. In addition, the relatively low C_{org}:N ratio for all seasons (ranged between 8.5 and 8.8) suggested a marine origin of the sinking particulate matter, in contrast to the C:N ratio greater than 20 found for organic matter from terrestrial sources (Emerson and Hedges, 1988). However, the direct comparison of C_{org} flux and primary production for the studied years did not result in a close relationship (r = 0.12), mainly due to the LU data with high primary production and low C_{org} fluxes (Fig. 8). This apparent decoupling between C_{org} flux and

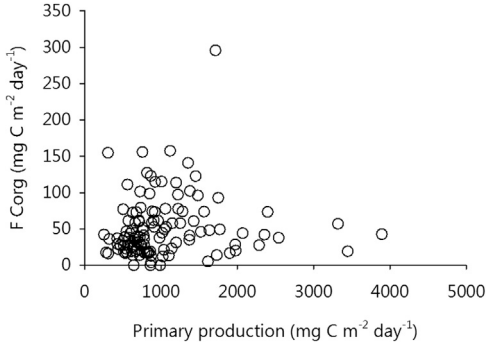

Fig. 8. Scatter plot of organic carbon fluxes at 300 m (mg C m^{-2} day^{-1}) vs. integrated primary production (mg C m^{-2} day^{-1}) during the period of sediment collection (usually two weeks).

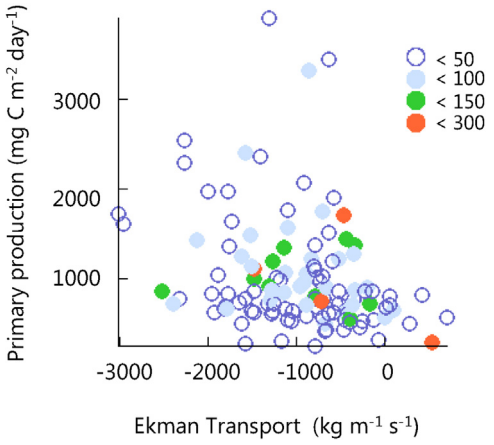

Fig. 9. Scatter plot of integrated primary production vs. Offshore Ekman transport (kg m^{-1} s^{-1}). Integrated primary production (mg C m^{-2} day^{-1}) and offshore Ekman transport values for each point correspond to the average of integrated primary production and across shore Ekman transport during the period of sediment collection (usually two weeks). Dot color scale represents the magnitude of organic carbon fluxes (mg C m^{-2} day^{-1}) for each sediment trap sample.

primary production suggests that other factors must influence C_{org} fluxes at depth. In fact, it is well established that strong upwelling-favorable, southward winds promote the formation of upwelling filaments in which large fractions of the biogenic particles from the continental shelf are transported offshore (Suess, 1980; Walsh, 1991; Thunell, 1998; Olli et al., 2001). Chavez et al. (2002) indicates that the productive area is extended offshore during the summer due to offshore flow in upwelling filaments. The seasonal variability in the vertical fluxes of C_{org} off Monterey Bay may be related to this transport, as follows (Fig. 9). Under strong offshore Ekman transport, rates of horizontal offshore export of the fixed organic carbon was high, often producing low vertical C_{org} fluxes, even in those situations with relatively high primary production. Stated simply, when Ekman transport is high, vertical export tends to be low (Fig. 9). In contrast, under weak offshore Ekman flow, horizontal export is low and vertical transport becomes more important, and more events with high C_{org} vertical fluxes were observed.

Zooplankton may also affect vertical fluxes of C_{org} by reprocessing material into fecal pellets. In his review of biological pump studies, Turner (2015) indicated that fecal pellets are often recycled in the upper few hundred meters of the water column by coprophagy and bacterial decomposition. Off Monterey Bay, maximum zooplankton abundance occurs during summer (Marinovic et al., 2002; Croll et al., 2005; Chavez et al., this issue). Consequently, maximum zooplankton feeding rates should be expected during the LU season, perhaps decoupling LU primary production peaks and reducing sinking C_{org} during this season.

In addition to seasonality, the study also spans very different interannual conditions, modulated by both local and large scale forcing (Chavez et al., 2011; Pennington and Chavez, in this issue). As previously pointed out, the region was strongly influenced by the strong 1997–1998 El Niño followed by an intense 1999–2000 La Niña period. After 2001, there was a strengthening of the California Current, reflected here by low salinity waters at station M2 (Fig. 2C), associated with an intensification of the North Pacific Gyre oscillation. Di Lorenzo et al. (2008) have shown that a positive North Pacific Gyre Oscillation indicates a strong Alaska Subpolar and North Pacific Subtropical Gyre, and strong California Current and coastal upwelling. This variability clearly affected the primary production of the Central California coastal upwelling system (Chavez et al., 2011), and to some extent, must be manifested in the interannual variability of C_{org} fluxes. Unfortunately, it was not possible to determine annual averages of C_{org} fluxes for the study years due to data gaps. Sampling coverage was less than 50% of the annual cycle for some study years, but it was possible to determine averages for the LU seasons for all the different years (Fig. 10). When C_{org} fluxes for the LU seasons of each year were compared, the lowest C_{org} fluxes occurred during years 1999, 2000 and 2001, in association with La Niña. In contrast, the C_{org} flux for the LU season of the 1998 El Niño year was similar to the C_{org} flux observed during 2002 through 2004. The LU seasons of 2003 and 2004 were characterized by an unusual onshore intrusion of the California Current, as also described for LU season of 1998 (Chavez et al., 2002; Collins et al., 2002). This anomalous shift of the California Current prevented the offshore horizontal transport of particulate organic matter present over the shelf, likely enhancing vertical export. In contrast, during La Niña years (1999, 2000 and 2001) intense upwelling-favorable winds enhanced horizontal export of particulate organic matter, likely reducing vertical C_{org} fluxes.

4.3. Attenuation of vertical organic carbon fluxes

Rapid biological consumption and remineralization of carbon in the mesopelagic zone (depths between the euphotic zone and 1000 m) reduce the flux carbon to depth (Buesseler et al., 2007). The comparison of vertical particle flux between the 300 m and 1200 m sediment traps provides an assessment of this vertical attenuation of sinking material. In this way, the 'efficiency' of the Central California coastal upwelling system in the transfer of organic carbon from the upper layers into the deep sea can be determined and thus the ability of this ecosystem to take up atmospheric CO_2 assessed.

Vertical attenuation of C_{org} fluxes was observed for all seasons except the LU. This vertical attenuation varied from 31% during the OC season to 24% for the DV season. These percentages are not high, revealing a system that efficiently moves organic carbon from the upper

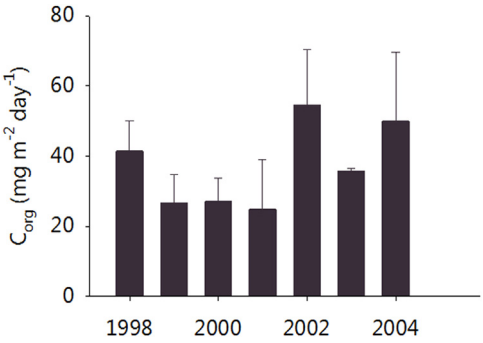

Fig. 10. Average C_{org} flux for each LU seasons (from May to July) during the seven study years.

layers with relatively little remineralization of organic carbon in the mesopelagic zone. Attenuation ranges were similar to those previously described by Buesseler et al. (2007) at the mesotrophic site of the Western Subarctic Gyre (43–53%) but are much lower than attenuation found at an oligotrophic site in the North Pacific Subtropical Gyre (~ 80%). The lower attenuation in the Subpolar Gyre was attributed to fast sinking of dense fecal pellets containing high proportions of ballasting biominerals, mainly biogenic silica.

The flux attenuation off Monterey Bay thus resembles that in the Subarctic Gyre and we hypothesize that similar controlling factors regulate flux. Off Monterey Bay, the phytoplankton community in the photic layer was mainly dominated by diatoms, which were the main contributors to the high primary production of the region (Pennington et al., 2010; Chavez et al., in this issue). Unfortunately, no biogenic silica data are available for the present sediment trap time series, but Monterey Bay measurements by Pilskaln et al. (1996) found high opal content. Silica was the largest contributor to biogenic material (average content of 17%) and had the highest correlation with C_{org} fluxes, supporting the idea that biogenic silica was the main ballast biomineral in this coastal upwelling system. In addition, Pilskaln et al. (1996) described an abundance of centric diatom valves within zooplankton fecal pellets in the sediment trap material during the upwelling months, suggesting a vertical C_{org} export mechanism similar to that described for the Western Subarctic Gyre (Honda et al., 2006; Buesseler et al., 2007).

Oxygen may also affect flux attenuation. Several authors (Devol and Hartnett, 2001; Van Mooy et al., 2002) suggested that low oxygen conditions greatly increase the amount of carbon transferred to the deep ocean due to decreased oxidation rate of the sinking material. Devol and Hartnett (2001) determined an attenuation of only 38% for the Mexican margin in comparison to 70% through a more typical oxic water column off Washington. Off Monterey Bay, a strong oxygen minimum with oxygen levels $< 20\ \mu mol\ kg^{-1}$ occurs between 500 m and 1000 m (Castro et al., 2001); conditions which could inhibit oxidation of sinking C_{org}. However, the water column between the two sediment traps also included well-ventilated upper waters, where heterotrophic activity and, consequently, oxidation of organic carbon takes place. Thus, the extent to which the presence of subtoxic waters may have inhibited degradation of sinking organic matter cannot be ascertained. Additional studies are necessary to unravel the role of low oxygen concentrations on the carbon transfer off Central California.

During the LU season, 41% higher C_{org} fluxes were observed at 1200 m than at 300 m. This large flux at the deepest trap remains enigmatic, but could have been due to lower efficiency of the shallower trap during this season (see Section 4.1) or to the collection of resuspended material. Sediments deposited on continental margins are prone to resuspension by vigorous bottom currents (Rea and Hovan, 1995). The strongest currents at both 300 and 1200 m off Monterey Bay occur during the LU season, being northward at 300 m and southward and offshore at 1200 m (Fig. 5C–E), producing the largest vertical shear. These dynamics could have resulted in resuspension and lateral offshore transport of slope sediment. Canyon sediment transport processes, such as slumping, turbidity flows and gravity flows are very active in the Monterey Canyon (Eittreim et al., 2002; Farnsworth and Milliman, 2003) and move sediment discharged from Salinas River oceanward (Paull et al., 2002; Xu et al., 2002). Alternatively, resuspended material could have been advected southwards from the Gulf of Farallones or by resuspension episodes similar to those documented at station M about 65 km southwest of Monterey Bay (Baldwin et al., 1998; Hwang et al., 2004). Hwang et al. (2010), based upon a compilation of C_{org} and ^{14}C of sinking material, estimated that 35% of C_{org} may derive from resuspended sediments globally, suggesting an important role of the resuspension of sedimentary organic matter and subsequent lateral transport in the export of organic carbon to the deep ocean. Further studies based on carbon isotope ratios are necessary to clarify the origin and impact of this resuspended material off Monterey Bay, considering also the potential contribution from sediment discharge from either the Salinas or Sacramento Rivers.

The ratio of particulate organic carbon to particulate inorganic carbon (C_{org}: C_{inorg}) of the exported material can also influence the carbon – sequestering efficiency of the biological pump (Tsunogai and Noriki, 1991; Wong et al., 1999; Antia et al., 2001; Honda et al., 2002), since carbon fixation by photosynthesis decreases and calcification have opposite effects on water column CO_2 (Tsunogai and Noriki, 1991; Frankignoulle et al., 1994). In contrast to photosynthesis, the formation of one mole of $CaCO_3$ releases approximately 0.6 mol of CO_2. Thus, the partial pressure of CO_2 is drawn down when photosynthesis exceeds $CaCO_3$ formation in surface waters (e.g. when C_{org}: $C_{inorg} > 0.6$ (Tsunogai and Noriki, 1991; Frankignoulle et al., 1994)). In this way, high C_{org}: C_{inorg} ratios indicate preferential carbon fixation as C_{org} rather than C_{inorg} favoring the biological pump as a mechanism for drawing atmospheric CO_2 into the ocean (Wong et al., 1999). For our sediment traps, the C_{org}: C_{inorg} ratio was relatively high, averaging 6.5 and 5.1 for 300 m and 1200 m, respectively, indicating that the study site acted as a sink of CO_2 on annual basis

Overall, the sediment trap data reveal an efficient transfer of organic carbon towards the sediment as supported by the relatively low attenuation of vertical fluxes for all seasons except late upwelling and the relatively high C_{org}: C_{inorg} ratio of sinking material at both 300 and 1200 m.

4.4. Seasonal POC budget for Monterey Bay

To summarize these results, a seasonal one dimensional (1D) vertical budget of C_{org} for Monterey Bay was produced (Fig. 11), using the measured primary production and vertical fluxes at 300 and 1200 m. In this way, the annual budget previously established by Pilskaln et al. (1996) was divided into seasons. Unfortunately, the photic zone export flux, i.e. the amount of C_{org} vertically exported from ~ 100 m, was not measured in spite of being a critical component of the C_{org} budget. Thus, these vertical fluxes have been estimated using published primary production and export flux observations in the California coastal upwelling region (Small et al., 1989; Pilskaln et al., 1996; Stukel et al., 2015). Calculated e-ratios, from these contemporary measurements of primary production and export flux, decrease with increasing primary production, as previously indicated by several authors (Pilskaln et al., 1996; Pennington et al., 2010; Stukel et al., 2013). Based on the best fit of e-ratio with primary production (PP) using the available data ($e\text{-ratio} = 6.425 \times PP^{-0.507}$ $r = 0.47$), the C_{org} flux at 100 m for each season was estimated. These 100 m fluxes accounted for between 25% and 18% of primary production, with maximum e-ratio values during the less productive DV season and a mean annual e-ratio of 0.19. Pilskaln et al. (1996) obtained the same e-ratio based on primary production and sediment trap data collected in Monterey Bay from 1989 through 1992 (see their Fig. 10).

In these seasonal 1D budgets, part of the export fluxes continues settling through the water column in such a way that the amount of C_{org} captured at the 300-m sediment trap constituted between 20% for the LU season and 32% for the EU and OC seasons of the estimated 100 m export fluxes, slightly higher than the annual mean of 18% obtained by Pilskaln et al. (1996). In terms of primary production, C_{org} flux at 300 m represented between 6.4% and 3.5% for the EU and LU seasons respectively. The lower percentage for the LU season must be due to either (1) increased horizontal export of material offshore in upwelling filaments or (2) intense heterotrophic processes between 100 m and 300 m (Section 4.2). Several authors have described maximum attenuation of vertical fluxes corresponding to this layer just above the oxycline (Martin et al., 1987; Antia et al., 2001; Henson et al., 2011). If the difference in C_{org} flux between 100 and 300 m was wholly due to heterotrophic processes, remineralization rates in this depth range varied from 117 $mg\ m^{-2}\ d^{-1}$ during the DV season to 171 $mg\ m^{-2}\ d^{-1}$ for LU season, not too different from the annual average of 177 $mg\ m^{-2}\ d^{-1}$

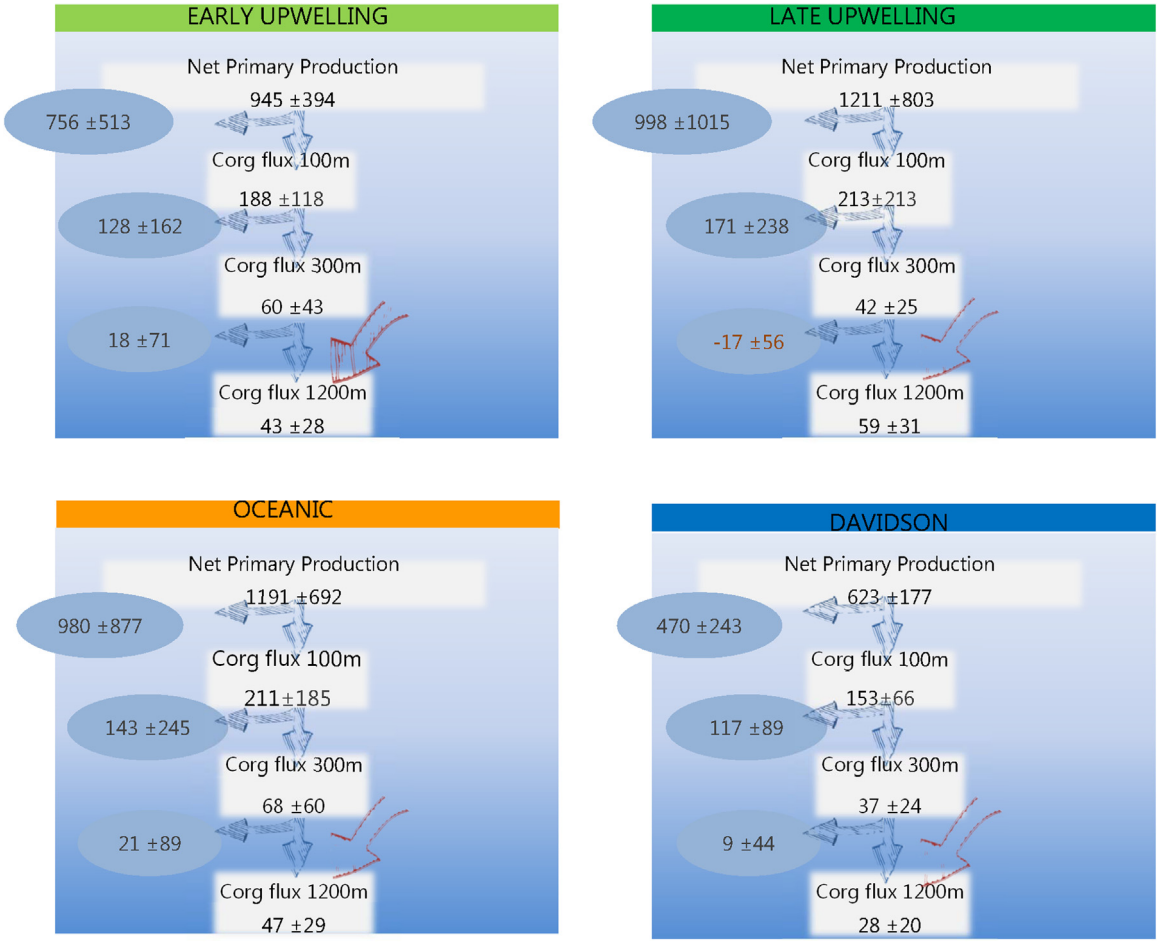

Fig. 11. Seasonal one dimensional budget of $C_{org,}$ mg m^{-2} day^{-1} for Monterey Bay. The brown arrow represents the potential lateral supply of resuspended material. EU is early upwelling, February to April, LU is late upwelling, May to July, OC is oceanic, August to October, and DV is Davidson season, November to January.

estimated by Pilskaln et al. (1996).

The organic carbon remineralization rates can be estimated from the difference between C_{org} fluxes for the two sediment trap depths. Excluding the LU season, when C_{org} flux at 1200 m was higher than C_{org} flux at 300 m, as previously discussed (Section 4.3), C_{org} remineralization rates varied between 9 mg m^{-2} d^{-1} during the DV season and 21 mg m^{-2} d^{-1} for the OC season. These values are somewhat lower than the average C_{org} remineralization rate (35.2–24.3 mg m^{-2} d^{-1}) estimated by Sonnerup et al. (2013) for the main thermocline of the NE Pacific based on oxygen utilization rates determined on isopycnals from 26.0 to 27.0 kg m^{-3} σ_θ and considering a respiration coefficient ranging from 1 to 0.7, respectively. In the present data, there seems to be a seasonal variability of deep-water remineralization affected by temperature. At higher average temperature during the OC season, C_{org} remineralization was higher and at a minimum during the DV season.

The C_{org} flux at 1200 m can be considered as the 'rain flux', i.e. the amount of C_{org} arriving at the surface sediment. Seasonal averages ranged between 28 mg m^{-2} d^{-1} for DV and 59 mg m^{-2} d^{-1} for LU. These values are higher than the average annual seafloor carbon flux of 19.7 mg m^{-2} day^{-1} reported by Pilskaln et al. (1996) based on benthic chamber and microelectrode measurements of oxygen, TCO_2 and carbonate alkalinity. However, our values were similar to the C_{org} rain to the seafloor of 34.8 and 45.6 mg m^{-2} d^{-1} derived by adding the oxidation rates and C_{org} burial rates used by Berelson and Stott (2003). The C_{org} fluxes at 1200 m also included seasonal variability with minimum values during the winter months reflecting minimum values of primary production during this season. For the four seasons, C_{org} flux at 1200 m represented about 4.0–4.9% of the primary production.

5. Conclusions

This study describes the flux of photosynthetically fixed organic carbon to the deep sea off Monterey Bay. On a seasonal scale, the vertical flux of C_{org} at 300 m represents around 3.5–6.4% of the fixed carbon. Low values of flux of C_{org} occur during the LU season from May to July, probably due to strong offshore Ekman transport and intense metabolic activity. The sediment trap data at 300 m and 1200 m allowed evaluation of the attenuation of C_{org} flux through the water column. Compared to other ecosystems, the attenuation of the vertical flux signal was relatively low for all seasons (24–31%), except during the LU season, pointing to a relatively unmodified and 'efficient' transfer of C_{org} through the mesopelagic layer by the biological pump. Excess C_{org} was collected in the 1200 m sediment trap during the LU season for unknown reasons. It is possible that strong deep currents may resuspend continental shelf or slope sediment, which is then advected offshore and captured by the trap. Unfortunately, it was not possible to estimate the percent contribution of the resuspended material even though such resuspension must be an important conduit of material to the deep ocean. The ratio of C_{org} flux at 1200 m to surface primary production was estimated to be 4.0–4.9%. These transfer efficiencies are in the upper range of previously reported values. In addition, the sinking material at 1200 m also presented relatively high C_{org}:C_{inorg} ratios. Thus, the analysis of the temporal time series of sinking particulate matter provided evidence that a strong biological pump in this coastal upwelling region efficiently sequesters atmospheric CO_2 in the deep sea.

In a changing ocean, coastal upwelling systems are critical regions

as they constitute the most biologically productive marine ecosystems. An increasing trend in water column stratification and a decrease in the intensity and frequency of coastal upwelling, as reported by recent investigations, could result in less upwelling of nutrient-rich upwelled water and a potential shift of the microbial community structure towards the dominance of the nano- and picoplankton. These potential changes in the ecosystem functioning could completely modify the fluxes of C_{org} to the deep ocean.

Acknowledgments

The principal source of support for these measurements was the David and Lucile Packard Foundation. CGC was partially supported by a National Research Council Fellowship at the Naval Postgraduate School. We would also like to acknowledge the efforts of the crew of the *R/V Point Sur* in setting and retrieving the sediment trap moorings. We would also thank to Marla Stone and Erich Rienecker for their capable assistance with sediment trap moorings, and Reiko Michisaki for help with computing. Comments from Drs Coale and Drinkwater and anonymous reviewers improved this paper considerably.

Appendix A. Supplementary material

Supplementary data associated with this article can be found in the online version at doi:10.1016/j.dsr2.2018.07.001.

References

Aguilar-Morales, J., 2003. Subtidal Circulation Over the Upper Slope to the West of Monterey Bay, California (Thesis). Naval Postgraduate School, Monterey, CA, pp. 128.

Antia, A.N., von Bodungen, B., Peinert, R., 1999. Particle flux across the mid-European continental margin. Deep Sea Res. Part I. 46 (12), 1999–2024.

Antia, A.N., Koeve, W., Fischer, G., Blanz, T., Schulz-Bull, D., Scholten, J., Neuer, S., Kremling, K., Kuss, J., Peinert, R., Hebbeln, D., Bathmann, U., Conte, M., Fehner, U., Zeitzschel, B., 2001. Basin-wide particulate carbon flux in the Atlantic Ocean: regional export patterns and potential for atmospheric CO_2 sequestration. Glob. Biogeochem. Cycles 15 (4), 845–862.

Asanuma, H., Rago, T.A., Collins, C.A., Chavez, F.P., Castro, C.G., 1999. Changes in the Hydrography of Central California Waters associated with the 1997–1998 El Niño. Technical Report NPS-OC-99-001. Naval Postgraduate School, Monterey, CA, pp. 121.

Baldwin, R.J., Glatts, R.C., Smith Jr., K.L., 1998. Particulate matter fluxes into the benthic boundary layer at a long time-series station in the abyssal NE Pacific: composition and fluxes. Deep Sea Res. Part II. 45 (4–5), 643–665.

Bauer, J., Cai, W.-J., Raymond, P.A., Bianchi, T.S., Hopkinson Jr, C.S., Regnier, P.A., 2013. The changing carbon cycle of the coastal ocean. Nature 504, 61–70.

Berelson, W.M., Stott, L.D., 2003. Productivity and organic carbon rain to the California margin seafloor: modern and paleoceanographic perspectives. Paleoceanography 18 (1) (2-1–2-15).

Buesseler, K.O., Antia, A.N., Chen, M., Fowler, S.W., Gardner, W.D., Gustafsson, O., Harada, H., Michaels, A.F., van der Loeff, M.R., Sarin, M., Steinberg, D.K., Trull, T., 2007. An assessment of the use of sediment traps for estimating upper ocean particle fluxes. J. Mar. Res. 65 (3), 345–416.

Carr, M.E., 2003. Simulation of carbon pathways in the planktonic ecosystem off Peru during the 1997–1998 El Niño and La Niña. J. Geophys. Res. 108 (C12), 3380.

Castro, C.G., Chavez, F.P., Collins, C.A., 2001. Role of the California undercurrent in the export of denitrified waters from the eastern tropical North Pacific. Glob. Biogeochem. Cycles 15 (4), 819–830.

Chavez, F., Messié, M., Pennington, J.T., 2011. Marine primary production in relation to climate variability and change. Ann. Rev. Mar. Sci. 3, 227–260.

Chavez, F.P., Pennington, J.T., Castro, C.G., Ryan, J.P., Michisaki, R.P., Schlining, B., Walz, P., Buck, K.R., McFadyen, A., Collins, C.A., 2002. Biological and chemical consequences of the 1997–1998 El Niño in central California waters. Prog. Oceanogr. 54 (1–4), 205–232.

Chavez, F.P., Sevadjian, J., Wahl, C., Friederich, J., Friederich, G.E., 2017. Measurements of pCO2 and pH from an autonomous surface vehicle in a coastal upwelling system. Deep Sea Res. Part II. https://doi.org/10.1016/j.dsr2.2017.01.001.

Chen, C.T.A., Borges, A.V., 2009. Reconciling opposing views on carbon cycling in the coastal ocean: continental shelves as sinks and near-shore ecosystems as sources of atmospheric CO_2. Deep Sea Res. Part II 56 (8–10), 578–590.

Collins, C.A., Castro, C.G., Asanuma, H., Rago, T.A., Han, S._K., Durazo, R., Chavez, F.P., 2002. Changes in the hydrography of Central California waters associated with the 1997–98 El Niño. Prog. Oceanogr. 54 (1–4), 205–232.

Collins, C.A., Pennington, J.T., Castro, C.G., Rago, T.A., Chavez, F.P., 2003. The California Current system off Monterey. California: physical and biological coupling. Deep Sea Res. Part II 50, 2389–2404.

Croll, D.A., Marinovic, B., Benson, S., Chavez, F.P., Black, N., Termullo, R., Tershy, R., 2005. From wind to whales: trophic links in a coastal upwelling system. Mar. Ecol. Prog. Ser. 289, 117–130.

De La Rocha, C.L., Passow, U., 2007. Factors influencing the sinking of POC and the efficiency of the biological carbon pump. Deep Sea Res. Part II 54 (5–7), 639–658.

Devol, A.H., Hartnett, H.E., 2001. Role of the oxygen-deficient zone in transfer of organic carbon to the deep ocean. Limnol. Oceanogr. 46 (7), 1684–1690.

Di Lorenzo, E., Schneider, N., Cobb, K.M., Franks, P.J.S., Chhak, K., Miller, A.J., McWilliams, J.C., Bograd, S.J., Arango, H., Curchitser, E., Powell, T.M., Rivière, P., 2008. North Pacific Gyre Oscillation links ocean climate and ecosystem change. Geophys. Res. Lett. 35, 8.

Ducklow, H.W., Steinberg, D.K., Buesseler, K.O., 2001. Upper ocean carbon export and the biological pump. Oceanography 14 (4), 50–58.

Eittreim, S.L., Xu, J.P., Noble, M., Edwards, B.D., 2002. Towards a sediment budget for the Santa Cruz shelf. Mar. Geol. 181 (1–3), 235–248.

Emerson, S., Hedges, J.I., 1988. Processes controlling the organic carbon content of open ocean sediments. Paleoceanography 3 (5), 621–634.

Falkowski, P.G., Flagg, C.N., Rowe, G.T., Smith, S.L., Whitledge, T.E., Wirick, C.D., 1988. The fate of a spring phytoplankton bloom: export or oxidation? Cont. Shelf Res. 8 (5–7), 457–484.

Farnsworth, K.L., Milliman, J.D., 2003. Effects of climatic and anthropogenic change on small mountainous rivers: the Salinas River example. Glob. Planet. Change 39 (1–2), 53–64.

Frankignoulle, M., Canon, C., Gattuso, J.-P., 1994. Marine calcification as a source of carbon dioxide: positive feedback of increasing atmospheric CO_2. Limnol. Oceanogr. 39 (2), 458–462.

Gardner, W.D., 1980. Field calibration of sediment taps. J. Mar. Res. 38, 41–52.

Gardner, W.D., 1985. The effect of tilt on sediment trap efficiency. Deep Sea Res. Part A. 32 (3), 349–361.

Gardner, W.D., Biscaye, P.E., Richardson, M.J., 1997. A sediment trap experiment in the Vema Channel to evaluate the effect of horizontal particle fluxes on measured vertical fluxes. J. Mar. Res. 55 (5), 995–1028.

Gruber, N., Sarmiento, J.L., 2002. Large scale biochemical/ physical interactions in elemental cycles. In: Robinson, A.R., McCarthy, J.J., Rothschild, B.J. (Eds.), The Sea: Biological-physical Interactions in the Oceans. John Wiley & Sons, New York NY, pp. 337–399.

Hansell, D.A., 2002. DOC in the global ocean carbon cycle. In: Hansell, D.A., Carlson, C.A. (Eds.), Biogeochemistry of Marine Dissolved Organic Matter. Academic Press, San Diego, pp. 685–715.

Henson, S.A., Sanders, R., Madsen, E., Morris, P.J., Le Moigne, F., Quartly, G.D., 2011. A reduced estimate of the strength of the ocean's biological carbon pump. Geophys. Res. Lett. 38 (4). https://doi.org/10.1029/2011GL046735.

Heussner, S., Durrieu de Madron, X., Calafat, A., Canals, M., Carbonne, J., Delsaut, N., Saragoni, G., 2006. Spatial and temporal variability of downward particle fluxes on a continental slope: lessons from an 8-yr experiment in the Gulf of Lions (NW Mediterranean). Mar. Geol. 234 (1–4), 63–92.

Honda, M.C., Imai, K., Nojiri, Y., Hoshi, F., Sugawara, T., Kusakabe, M., 2002. The biological pump in the northwestern North Pacific Ocean based on fluxes and major components of particulate matter obtained by sediment-trap experiments (1997–2000). Deep Sea Res. Part II 49 (24–25), 5595–5625.

Honda, M.C., Kawakami, H., Sasaoka, K., Watanabe, S., Dickey, T., 2006. Quick transport of primary produced organic carbon to the ocean interior. Geophys. Res. Lett. 33, 16.

Honjo, S., Doherty, K.W., 1988. Large aperture time-series sediment traps; design objectives, construction and application. Deep Sea Res. Part A 35 (1), 133–149.

Hopkinson Jr, C.S., Vallino, J.J., 2005. Efficient export of carbon to the deep ocean through dissolved organic matter. Nature 433 (13), 142–145.

Hwang, J., Druffel, E.R.M., Griffin, S., Smith Jr., K.L., Baldwin, R.J., Bauer, J.E., 2004. Temporal variability of $\Delta^{14}C$, $\delta^{13}C$, and C/N in sinking particulate organic matter at a deep time series station in the northeast Pacific Ocean. Glob. Biogeochem. Cycles 18 (4), 9.

Hwang, J., Druffel, E.R.M., Eglinton, T.I., 2010. Widespread influence of resuspended sediments on oceanic particulate organic carbon: insights from radiocarbon and aluminum contents in sinking particles. Glob. Biogeochem. Cycles 24 (GB4016).

Inthorn, M., Wagner, T., Scheeder, G., 2006. Lateral transport controls distribution, quality, and burial of organic matter along continental slopes in high-productivity areas. Geology 34 (3), 205–208.

IPCC, 2013. Climate change 2013: the physical science basis. In: Stocker, T.F., Qin, D., Plattner, G.-K., Tignor, M.M.B., Allen, S.K., Boschung, J., Nauels, A., Xia, Y., Bex, V., Midgley, P.M. (Eds.), Working Group I Contribution to the Fifth Assessment Report of the Intergovernmental Panel on Climate Change. Cambridge University Press, Cambridge, pp. 1535.

Lampitt, R.S., Achterberg, E.P., Anderson, T.R., Hughes, J.A., Iglesias-Rodríguez, M.D., Kelly-Gerreyn, B.A., Lucas, M., Popova, E.E., Sanders, R., Shepherd, J.G., Smythe-Wright, D., Yool, A., 2008. Ocean fertilization: a potential means of geoengineering? Philos. Trans. R. Soc. A 366, 3919–3945.

Carbon and nutrient fluxes in continental margins. In: Liu, K.-K., Atkinson, L., Quiñones, R., Talaue-McManus, L. (Eds.), 2010. Global Change. Springer-Verlag Berlin, Heidelberg.

Marinovic, B.B., Croll, D.A., Gong, N., Benson, S.R., Chavez, F.P., 2002. Effects of the 1997–1999 El Niño and La Niña events on zooplankton abundance and euphausiid community composition within the Monterey Bay coastal upwelling system. Prog. Oceanogr. 54 (1–4), 265–277.

Martin, J.H., Knauer, G.A., Karl, D.M., Broenkow, W.W., 1987. VERTEX: carbon cycling in the northeast Pacific. Deep Sea Res. Part A 34 (2), 267–285.

Muller-Karger, F.E., Varela, R., Thunell, R., Luerssen, R., Hu, C., Walsh, J.J., 2005. The importance of continental margins in the global carbon cycle. Geophys. Res. Lett. 32

(1), 1–4.
Olli, K., Riser, C.W., Wassmann, P., Ratkova, T., Arashkevich, E., Pasternak, A., 2001. Vertical flux of biogenic matter during a Lagrangian study off the NW Spanish continental margin. Prog. Oceanogr. 51 (2–4), 443–466.
Passow, U., Carlson, C.A., 2012. The biological pump in a high CO_2 world. Mar. Ecol. Prog. Ser. 470, 249–271.
Paull, C.K., Greene, H.G., Ussler, W., Mitts, P.J., 2002. Pesticides as tracers of sediment transport through Monterey Canyon. Geo-Mar. Lett. 22, 121–126.
Pennington, J.T., Chavez, F.P., 2000. Seasonal fluctuations of temperature, salinity, nitrate, chlorophyll and primary production at station H3/M1 over 1989–1996 in Monterey Bay, California. Deep Sea Res. Part II. 47, 947–973.
Pennington, J.T., Castro, C.G., Collins, C.A., Evans, W.W.I., Friederich, G.E., Michisaki, R.P., Chavez, F.P., 2010. A carbon budget for the northern and central California coastal upwelling system. In: Liu, K.-K., Atkinson, L., Quiñones, R., Talaue-NcManus, L. (Eds.), Carbon and Nutrient Fluxes in Continental Margins. Global Change. Springer-Verlag, Berlin, Heidelberg, pp. 29–44.
Pennington, T.P., Chavez, F.P., 2017. Decade-scale oceanographic fluctuation in Monterey Bay, California, 1989–2011. Deep Sea Res. Part II. https://doi.org/10.1016/j.dsr2.2017.07.005.
Peterson, M.L., Hernes, P.J., Thoreson, D.S., Hedges, J.I., Lee, C., Wakeham, S.G., 1993. Field evaluation of a valved sediment trap. Limnol. Oceanogr. 38 (8), 1741–1761.
Pilskaln, C.H., Paduan, J.B., Chavez, F.P., Andereson, R.Y., Berelson, W.M., 1996. Carbon export and regeneration in the coastal upwelling system of Monterey Bay, central California. J. Mar. Res. 54, 1149–1178.
Rea, D.K., Hovan, S.A., 1995. Grain size distribution and depositional processes of the mineral component of abyssal sediments: lessons from the North Pacific. Paleoceanography 10 (2), 251–258.
Riebesell, U., Körtzinger, A., Oschlies, A., 2009. Sensitivities of marine carbon fluxes to ocean change. Proc. Natl. Acad. Sci. USA 106 (49), 20602–20609.
Sakamoto, C.M., Friederich, G.E., & Codispoti, L.A., 1990. MBARI procedures for automated nutrient analysis using a modified Alpkem Series 300 rapid flow analyzer. Monterey Bay Aquarium Research Institute Technical Report No. 90–92, Monterey Bay Aquarium Research Institute, Moss Landing, CA, 84 pp.
Schwing, F., O'Farreu, M., Steger, J. Baltz, K., 1996. Coastal upwelling indices, West Coast of North America, 1946–1955. US. Department of Commerce, NOAA Technical Memorandum NOAA-TM-NMFS-SWFS-231, La Jolla, California, 207 pp.
Sigman, D.M., Boyle, E.A., 2000. Glacial/interglacial variations in atmospheric carbon dioxide. Nature 407, 859–869.
Small, L.F., Landry, M.R., Eppley, R.W., Azam, F., Carlucci, A.F., 1989. Role of plankton in the carbon and nitrogen bubgets of Santa Monica Basin, California. Mar. Ecol. Prog. Ser. 56 (1–2), 57–74.
Sonnerup, R.E., Mecking, S., Bullister, J.L., 2013. Transit time distributions and oxygen utilization rates in the Northeast Pacific Ocean from chlorofluorocarbons and sulfur hexafluoride. Deep Sea Res. Part I 72, 61–71.
Steinberg, D.K., Van Mooy, B.A.S., Buesseler, K.O., Boyd, P.W., Kobari, T., Karl, D.M., 2008. Bacterial vs. zooplankton control of sinking particle flux in the ocean's twilight zone. Limnol. Oceanogr. 53 (4), 1327–1338.
Strub, P.T., Allen, J.S., Huyer, A., Smith, R.L., Beardsley, R.C., 1987. Seasonal cycles of currents, temperatures, winds, and sea level over the Northeast Pacific continental shelf: 35°N to 48°N. J. Geophys. Res. 92 (C2), 1507–1526.
Stukel, M.R., Ohman, M.D., Benitez-Nelson, C.R., Landry, M.R., 2013. Contributions of mesozooplankton to vertical carbon export in a coastal upwelling system. Mar. Ecol. Prog. Ser. 491, 47–65.
Stukel, M.R., Kahru, M., Benitez-Nelson, C.R., Décima, M., Goericke, R., Landry, M.R., Ohman, M.D., 2015. Using Lagrangian-based process studies to test satellite algorithms of vertical carbon flux in the eastern North Pacific Ocean. J. Geophys. Res. 120 (11), 7208–7222.
Suess, E., 1980. Particulate organic carbon flux in the oceans - surface productivity and oxygen utilization. Nature 288, 260–262.
Thunell, R., Benitez-Nelson, C., Varela, R., Astor, Y., Muller-Karger, F., 2007. Particulate organic fluxes along upwelling-dominated continental margins: rates and mechanisms. Glob. Biogeochem. Cycles 21 (101029/102006GB002793).
Thunell, R.C., 1998. Particle fluxes in a coastal upwelling zone: sediment trap results from Santa Barbara Basin California. Deep Sea Res. Part I 45, 1863–1884.
Thunell, R.C., Varela, R., Llano, M., Collister, J., Muller-Karger, F., Bohrer, R., 2000. Organic carbon fluxes, degradation and accumulation in an anoxic basin: sediment trap results from the Cariaco Basin. Limnol. Oceanogr. 45 (2), 300–308.
Tsunogai, S., Noriki, S., 1991. Particulate fluxes of carbonate and organic carbon in the ocean. Is the marine biological activity working as a sink of the atmospheric carbon? Tellus 43 (2), 256–266.
Turner, J.T., 2015. Zooplankton fecal pellets, marine snow, phytodetritus and the ocean's biological pump. Prog. Oceanogr. 130, 205–248.
Van Mooy, B.A.S., Keil, R.G., Devol, A.H., 2002. Impact of suboxia on sinking particulate organic carbon: enhanced carbon flux and preferential degradation of amino acids via denitrification. Geochim. Cosmochim. Acta 66 (3), 457–465.
Volk, T., Hoffert, M.I., 1985. Ocean carbon pumps: analysis of relative strengths and efficiencies in ocean-driven atmospheric CO_2 changes. In: Sundquist, E.T., Broecker, W.S. (Eds.), The Carbon Cycle and Atmospheric CO_2: Natural variations Archaean to Present. Geophysical Monographs 32. American Geophysical Union, Washington, D.C., pp. 99–110.
Walsh, J.J., 1991. Importance of continental margins in the marine biogeochemical cycling of carbon and nitrogen. Nature 350 (6313), 53–55.
Wong, C.S., Whitney, F.A., Crawford, D.W., Iseki, K., Matear, R.J., Johnson, W.K., Page, J.S., Timothy, D., 1999. Seasonal and interannual variability in particle fluxes of carbon, nitrogen and silicon from time series of sediment traps at Ocean Station P, 1982–1993: relationship to changes in subarctic primary productivity. Deep Sea Res. Part II 46 (11–12), 2735–2760.
Xu, J.P., Noble, M., Eittreim, S.L., Rosenfeld, L.K., Schwing, F.B., Pilskaln, C.H., 2002. Distribution and transport of suspended particulate matter in Monterey Canyon. California. Mar. Geol. 181 (1–3), 215–234.